revista Matéria

ISSN 1517-7076

Revista Matéria, v. 16, n. 3, pp. 747 – 753, 2011
http://www.materia.coppe.ufrj.br/sarra/artigos/artigo11434

Precipitation reaction in alpha-Cu-Al-Ag alloys

R.A.G. SILVA [I], A.T. ADORNO[II], T.M. CARVALHO[II], A.G. MAGDALENA[II], C.M.A. SANTOS[II]

[I] UNIFESP, Departamento de Ciências Exatas e da Terra, 09920-540 – Diadema-SP.
e-mail: galdino.ricardo@gmail.com
[II] Instituto de Química-UNESP, Departamento de Físico-Química, Laboratório de Materiais Metálicos, Caixa Postal 355, 14801-970 Araraquara-SP.
e-mail: atadorno@iq.unesp.br ; thaisa.mary@gmail.com ; aroldogm@gmail.com ; camilaandr@gmail.com

ABSTRACT

The Ag-rich precipitates formation reaction in the Cu-9.22%at. Al-4.66%at. Ag, Cu-9.31%at. Al-5.83%at. Ag and Cu-9.37%at. Al-7.08%at. Ag alloys was studied using microhardness change measurements with temperature and time, differential scanning calorimetry (DSC), scanning electron microscopy (SEM) and X-ray diffractometry (XRD). The results indicated that the Ag-rich phase formation is an interface controlled process with a zero-order mechanism, due to the amount of unsolved Ag that makes the precipitation reaction rate independent of Ag concentration.

Keywords: Ag additions, Cu-based alloys, kinetics.

1 INTRODUCTION

In the growth of precipitates from supersaturated solid solutions, the rate of growth depends upon the rate at which atoms are brought to, or removed from, the interface by diffusion and the rate at which they cross the interface. During the early stage of growth the interface reaction must be the slower of these steps because of the limited area of interface and because the distance over which diffusion is necessary tends to zero. At large particle sizes the reverse is true because the diffusional flux gets progressively slower due to the continuous removal of solute from solution reducing the concentration gradient which is the driving force for diffusion, whilst the flux across the interface increases due to the increase in area [1].

According to the Cu-Al equilibrium diagram [2, 3], the α-Cu solid solution limit is between 17.97 % at. and 18.91 % at. Al below 300 °C. In this way, α-(Cu-Al) alloys in this field are not susceptible to age hardening. Silver additions to Cu-Al alloys increase its hardness [4], corrosion resistance [5], and modify the aging characteristics of the alloys [6]. Phases in Cu-Al-Ag alloys are structurally analog to those present in the binary systems, without ternary intermediary phases [7, 8, 9]. In Cu-Al-Ag alloys the Ag-rich phase formation follows a growth and nucleation mechanism influenced by Ag content [10].

In this work, the Ag rich phase formation in the Cu-9.22%at. Al-4.66%at. Ag, Cu-9.31%at. Al-5.83% at. Ag and Cu-9.37% at. Al-7.08% at. Ag alloys was studied using differential scanning calorimetry (DSC), microhardness change measurements with temperature and time, scanning electron microscopy (SEM) and X-ray diffractometry (XRD).

2 MATERIALS AND METHODS

The Cu-9.22 % at. Al-4.66 % at. Ag, Cu-9.31 % at. l-5.83%at. Ag and Cu-9.37 % at. Al-7.08 % at. Ag alloys were prepared in an induction furnace under argon atmosphere using 99.95% copper, 99.97% aluminum and 99.98% silver as starting materials. Results from chemical analysis indicated a final alloys composition very close to the nominal one, with Pb, Fe, and Mn as main impurities (concentration less than 100 ppm). Cylindrical samples with 2.0 cm diameter and 6.0 cm length were cut in disks of 2.0 mm thickness. The disks were cold rolled and flat squares samples of 1.0 mm thickness and about 5.0 mm length were used for hardness measurements and scanning electron microscopy. Previous results [6] indicated that the Ag dissolution occurs at about 780°C, therefore the samples were solution treated at a higher temperature. All samples were annealed during 120 h at 850 °C for homogenization, and some of them were then equilibrated for 1 h at 850 °C and quenched in iced water to maintain Ag in solution. Some of the quenched samples were equilibrated for 1 h at temperatures ranging from 100 to 900 °C and quenched in iced water,

Autor Responsável: R. A. G. SILVA   Data de envio: 21/01/11   Data de aceite: 26/09/11

thus characterizing an isochronic process. Other samples, quenched from 850 °C in iced water, were aged at five different temperatures chosen at about the maximum Ag precipitation temperature, determined from DSC measurements and hardness measurements on the aged samples gave the hardness/ageing time curves. After the heat treatments the samples were polished, etched and examined by SEM using a Jeol JSM T330A. The XRD diagrams were obtained using a Siemens D5000 4B diffractometer, Cu Kα radiation and solid (not powdered) samples. DSC curves were obtained using a Q20 TA Instruments and the Vickers hardness measurements were made with a Buehler Micromet 2003 Microhardness Tester using a load of 0.5 kg. Each hardness number was calculated from an average of 10 hardness impressions with a standard deviation of about 2%.

3 RESULTS AND DISCUSSION

Figure 1-a shows the DSC curves obtained with a heating rate of 20°C.min^{-1} for samples initially quenched and Figure 1-b shows the plot of hardness values vs. isochronic quenching temperature obtained for the Cu-9.22%at. Al-4.66%at. Ag, Cu-9.31%at. Al-5.83%at. Ag and Cu-9.37%at. Al-7.08%at. Ag alloys. In the DSC curves of Figure 1-a one can observe an exothermic peak at the temperature range from 475 to 575 ^{o}C. This thermal event is associated with Ag precipitation retained by quenching [10]. In the curves of Figure 1-b it is possible to observe that the alloy hardness increases with isochronic quenching temperature and with the silver content. All alloys show a hardness maximum at about 450 ^{o}C. Considering that the studied alloys are in the Cu-rich corner (α field) of the Cu-Al–Ag system [9], it is possible to attribute the hardness peaks to Ag precipitation. This was confirmed by the XRD patterns shown in Figure 2 and by the micrographs in Figure 3. These micrographs show that after quenching from 300 °C (Figure 3-a) there are silver precipitates at the grain boundaries and after quenching from 450 ^{o}C (Figure 3-b) the Ag precipitates fraction is increased.

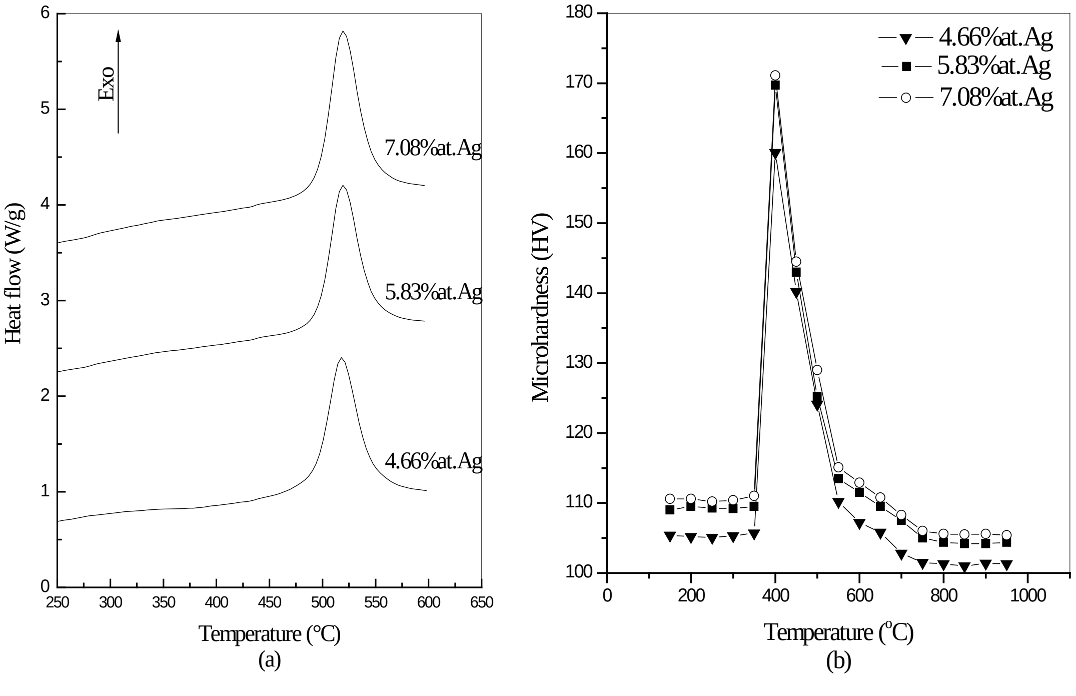

Figure 1: (a) DSC curves obtained with a heating rate of 20 ^{o}Cmin^{-1} for samples initially quenched from 850 ^{o}C (b) Plots of microhardness changes vs. isochronic quenching temperature.

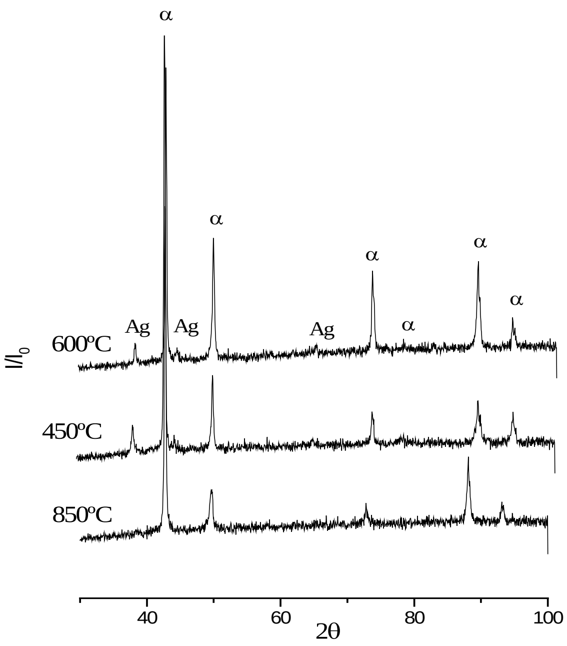

Figure 2: X-ray diffraction patterns obtained for the Cu-9.22%at. Al-4.66%at. Ag alloy initially quenched from 850 ^{o}C.

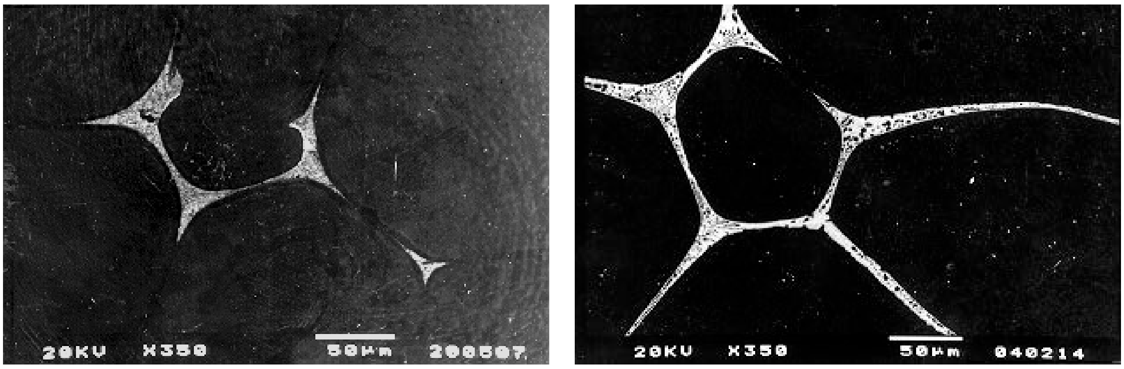

(a) (b)

Figure 3: Scanning electron micrographs (BEI) obtained for the Cu-9.37%at. Al- 7.08%at. Ag alloy: (a) quenched from 300 ^{o}C; (b) quenched from 450°C.

The thermal behavior of α-Cu–Al–Ag alloys, or those with Al content up to 17.97at.%, when compared with other systems, e.g. Cu–Be–Mg, shows some interesting features. α-Cu–Al alloys show no thermal events due to the complete Al solubility in this range, while α-Cu–Al–Ag alloys show a new thermal event due to Ag dissolution or precipitation (see Figure 1-a and 1-b). This behavior is ascribed to the weak interaction (small electronegativity difference) between Cu and Ag atoms. On the other hand, the Cu–Be system shows four thermal events, which are disturbed by the presence of Mg, due to the strong interaction between Mg atoms and vacancies [11]. It is known that the fraction of particles in a system having energy E is proportional to the Boltzmann factor $e^{-Ea/RT}$. The number of particles taking part in a reaction has to surmount the activation energy barrier and, in this way, the Boltzmann factor may be associated with the reaction rate [1]. Hence, considering that with the increase in the quenching temperature the Ag atoms fraction that precipitates during the isochronal process is increased, its maximum value may be associated with the major possible fraction of precipitates formed at constant time. So, the hardness peak in Figure 1-b may indicate that the maximum rate for precipitation reaction is at about the temperature corresponding to this maximum. The maximum for all curves in Figure 1-b is at about 450°C and the precipitation process is also close to a maximum at this temperature. A more precise indication of this maximum temperature is given by the DSC curves in Figure 1-a, where one can verify that the reaction maximum is at about 500 °C. The aging temperatures were then selected up to this maximum and all studied alloys were aged at 300, 350, 400, 450 and 500°C. This was due considering that for transformations in metals and alloys involving a change from a high temperature phase to a low temperature phase during isothermal annealing the reaction, once started, proceeds slowly both at high temperature near to the transition temperature and at low temperatures [12]. Figure 4-a shows the isothermal hardness vs. aging time curves for alloys aged at 450 °C. Similar curves were obtained for all studied alloys at the selected aging temperatures. It is possible to verify that age hardening occurred in all alloys with silver additions, providing evidence that (a) the hardness increase was always preceded by an incubation period, the magnitude of which depends on the aging temperature and on the silver content and (b) there is little variation of the peak-hardness values with the aging temperature for each alloy.

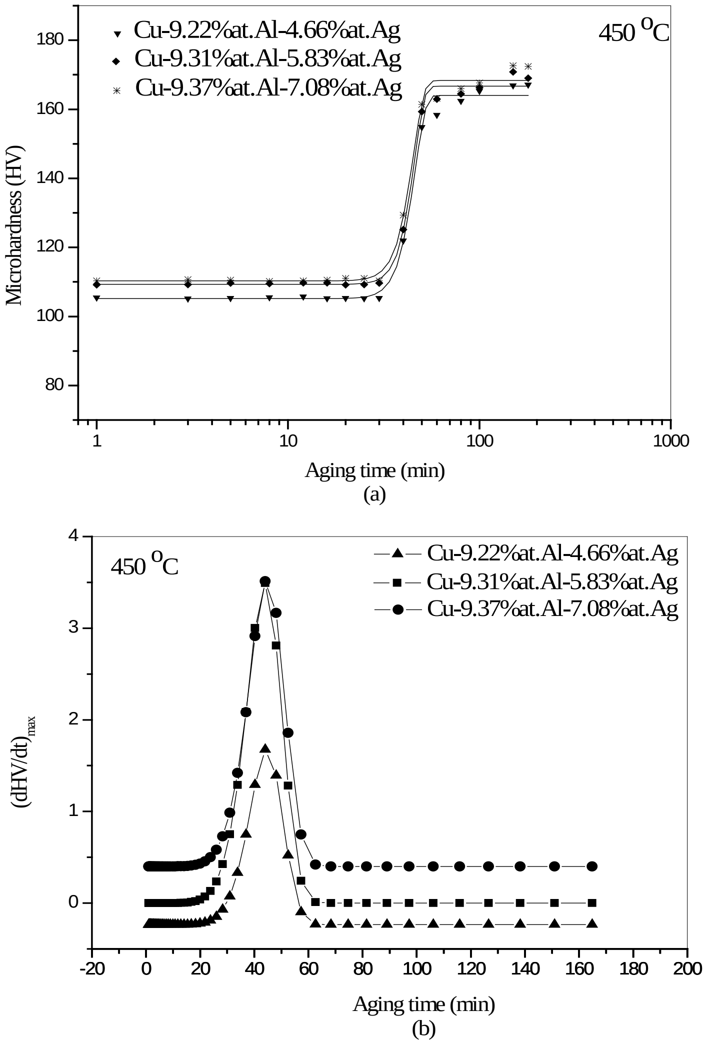

(a)

(b)

Figure 4: (a) Plots of microhardness changes vs. aging time and (b) Plots of dHV/dt vs. aging time.

The sigmoidal curves in Figure 4-a may be associated with changes in the transformed fraction with time for the Ag precipitation reaction and the derivative of these curves, $(\partial HV/\partial t)_T$ or the hardening rate at constant temperature, may correspond to the precipitation reaction rate. Figure 4-b shows the hardening rate vs. time curves obtained for alloys aged at 450 °C. From this figure and from similar curves obtained at the other aging temperatures, one can observe that the hardening rate is increased up to a maximum value and then decreases down to values close to those initially obtained. This initial raise can be due to the increase of growth rate and the subsequent decrease to a growth rate decrease of Ag precipitates. The transformed fraction vs. time curves, in Figure 4-a, show an induction or incubation period that can be related to the nucleation process and, in this case, corresponds to silver-rich nuclei formation. During this period, nucleation is the dominant process and the growth of silver-rich precipitates starts to dominate at the end of the incubation period. This is evidenced by the hardness increase, and also indicates that in this case nucleation and growth can be interpreted as consecutive processes. Then, one can consider that after the end of the incubation period the nuclei grow continuously and any dimension of the transformed region is a linear function of time. This corresponds to an almost linear hardness change with time at a constant temperature. The growth rate reduction, observed from the inflection point of Figure 4-a and evidenced by the derivative curve in Figure 4-b after the maximum, is due to the mutual impingement of regions transforming from separate nuclei[12], and is also possibly due to coarsening and to the slowest silver diffusion from bulk to grain boundary. In this way, the maximum in Figure 4-b can be associated with the maximum rate of Ag precipitation from the matrix.

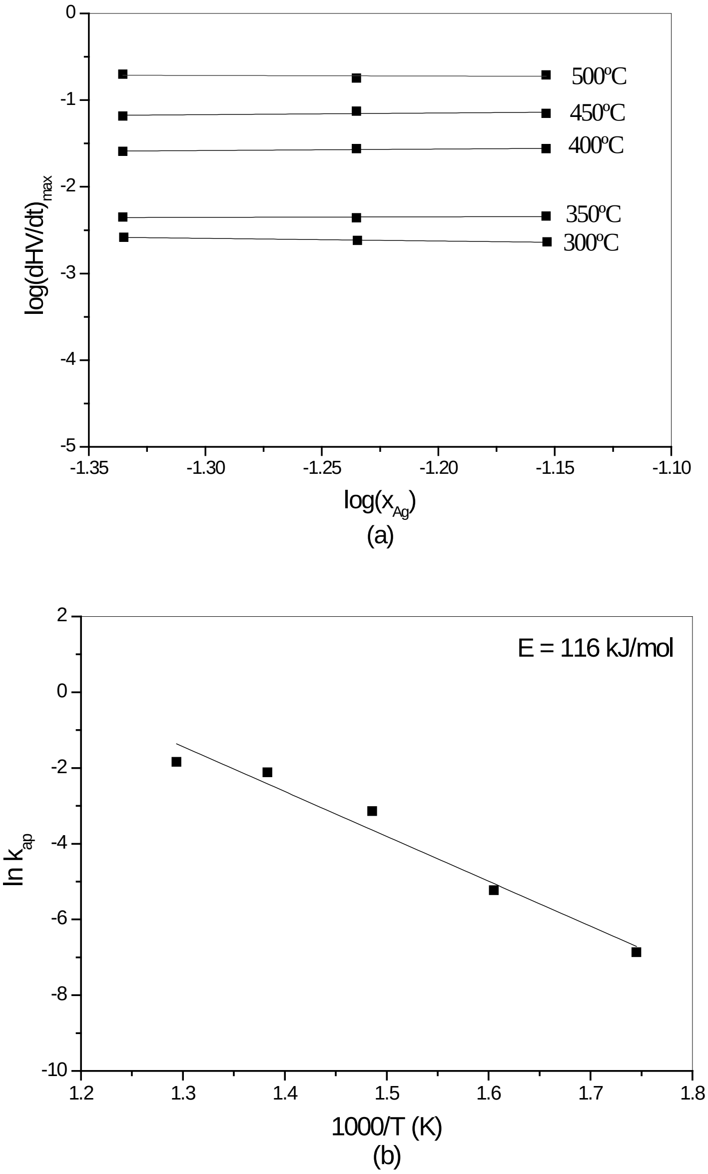

Figure 5: (a) Plots of log $(dHV/dt)_{max}$ vs. log x_{Ag} obtained at the temperature range from 300 to 500 °C and (b) Plots of ln k_{ap} vs. 1000/T.

From what was proposed in the discussion of Figure 4-b, the rate equation for the Ag precipitation reaction, which is associated with the precipitates growth, may be written as

$$\frac{dHV}{dt} = k_{ap}[Ag]^n \qquad (1)$$

or

$$\log \frac{dHV}{dt} = n \log[Ag] + \log k_{ap} \tag{2}$$

Substitution of the reaction rate maxima at each aging temperature and the corresponding (x_{Ag}) Ag mole fraction values, for all studied alloys, in Eq. (2) gives the linear plots shown in Figure 5-a, with slope corresponding to the precipitation reaction order (n) and linear coefficient corresponding to the apparent rate constant k_{ap}. The obtained values for n and k_{ap} are shown in Table 1.

From this approach one may observe that Fig 5-a, corresponding to the temperatures of 300, 350, 400, 450 and 500°C, indicates a zero-order reaction for all Ag concentrations. Considering that the Boltzmann factor may be associated with the reaction rate, the dependence of k_{ap} with T may be described by the Arrhenius equation

$$k_{ap} = k_o \exp\left(\frac{-E_a}{R\,T}\right) \tag{3}$$

where k_o is the pre-exponential factor, E_a is the activation energy for the precipitation process and R is the gas constant. Figure 5-b shows the plot of ln k_{ap} vs. *1000/T*. The activation energy values obtained for the zero-order process was E_a = 116.0 kJ/mol.

Table 1: Values of the reaction order (n) and kinetic constant (k_{ap}).

Temperature	300 °C	350 °C	400 °C	450 °C	500 °C
n	0	0	0	0	0
$k_{ap}/10^{-3}$	2.69	4.47	25.6	65.2	199

The Ag solubility limit for α-(Cu–Al) alloys is at about 6wt% [13] and is greater than the Ag solubility in pure copper. This greater solubility may be associated with the presence of Al, whose chemical affinity with Ag is greater than the corresponding Cu–Ag affinity. For the Cu-9.22%at. Al-4.66%at. Ag, Cu-9.31%at. Al-5.83%at. Ag and Cu-9.37%at. Al-7.08%at. Ag alloys, the amount of unsolved Ag provides a source of available Ag atoms that makes the precipitation reaction rate independent of Ag concentration. This reaction mechanism is ascribed to the lower chemical potential in the system due to the unsolved Ag, which decreases the diffusion path to grain boundaries of the Cu-rich matrix. Due to this lower chemical potential, the amount of Ag atoms dragged to grain boundaries is almost the same for all alloys and hence the diffusive process is practically independent of Ag concentration at each sample, or the reaction is of zero order. The higher activation energy value obtained for this zero-order process, when compared with that obtained for the Cu-6 % wt. Al with Ag additions [10], seems to indicate a relation between the activation energy and Al content. This was expected considering that the lower Al concentration can decrease Ag dissolution into α-(Cu-Al) matrix, thus increasing the unsolved Ag fraction. This great amount of unsolved Ag will correspond to Ag saturation at the precipitate interface and to a lower chemical potential in this region, thus leading to a lower jump frequency and to higher activation energy. This suggests that the interfacial process is dominant in the Ag-rich phase formation.

4. CONCLUSIONS

The results indicated that the Ag precipitation reaction in Cu-9.22%at. Al-4.66 % at. Ag, Cu-9.31 % at. Al-5.83 % at. Ag and Cu-9.37 % at. Al-7.08%at. Ag alloys corresponds to a zero-order reaction. This indicates a constant Ag diffusion rate at each studied sample in the considered temperature range, which was attributed to the characteristics of the Cu-Al-Ag system. The results also showed that the Ag-rich phase formation is an interface- controlled process.

5. ACKNOWLEDGEMENTS

The authors thank the support of FAPESP (Project no. 2006/0418-0), CNPq and CAPES.

6. REFERENCES

[1] BURKE, J., *The kinetic of phase transformations in metals*; Oxford: Pergamon Press; 1965.

[2] MASSALSKI, T.B., *Binary Alloy Phase Diagrams*, 2nd ed., Ohio: American Society for Metals; 1992.

[3] LIU, X.J., OHNUMA, I, KAINUMA, R., ISHIDA, K., “Phase equilibra in the Cu-rich portion of the Cu-Al binary system”, *Journal of Alloys Compounds*, v. 264, n. 1-2, pp. 201-208, 1998.

[4] ADORNO, A.T., CILENSE, M., GARLIPP, W., “Mechanical properties and precipitation energy of the copper-5,4% aluminum-5,2% silver alloy”, *Journal of Materials Science Letters*, v. 6, n. 2, pp. 163-164, 1987.

[5] ROSATTO, S.S., CABOT, P.L., SUMODJO, P.T.A., BENEDETTI, A.V., “Electrochemical studies of copper-aluminun-silver alloys in 0.5M H_2SO_4”, *Electrochimica Acta*, v. 46, n. 7, pp. 1043-1051, 2001.

[6] ADORNO, A.T., SILVA, R.-A.-G., “Kinetics of Ag-rich precipitates formation in Cu–Al–Ag alloys”, *Materials Science and Engineering A*, v. 374, pp. 170–176, 2004.

[7] MASSALSKI, T.B., PEREPEZKO, J.H., “Constitution and phase relationship in copper-silver-aluminumternary-system”, *Zeitschrift fur Metallkunde*, v. 64, n. 3, pp. 176-181, 1973.

[8] ADORNO, A.T., SILVA, R.A.G., “Effect of 4mass%Ag addition on the thermal behavior of the Cu-9mass%Al alloy”, *Journal of Thermal Analysis and Calorimetry*, v. 73, n. 3, pp. 931-938, 2003.

[9] WITUSIEWICZ, V.-T., HECHT, U., FRIES, S.-G., REX, S., “The Ag-Al-Cu system II. A thermodynamic evaluation of the ternary system”, *Journal of Alloys and Compounds*, v. 387, pp. 217-227, 2005.

[10] CARVALHO, T.M., ADORNO, A.T., SILVA, R.A.G., “Ag-rich phase formation in the Cu-6wt%Al alloy with Ag additions”, *Journal of Physics and Chemistry of Solids*, v. 69, n. 8, pp. 2025-2031, 2008.

[11] DONOSO, E., VARSCHAVSKY, A., “Microcalorimetric evaluation of precipitation in Cu-2Be-0.2Mg”, *Journal of Thermal Analysis and Calorimetry*, v. 63, pp. 249-266, 2001.

[12] CHRISTIAN, J.W., *The theory of transformations in metals and alloys Part 1*, 3rd ed., Oxford: Pergamon Press, 2002.

[13] ADORNO, A.T., BEATRICE, C.R.S., BENEDETTI, A.V., CABOT, P.L., “Silver dissolution on copper-based alloys”, *Journal of Materials Science*, v. 28, pp. 411-414, 1993.